Complex-cubic Ginzburg–Landau equation-based model for erbium-doped fiber-amplifier-supported nonreturn-to-zero communications

Nikos Efremidis and Kyriakos Hizanidis

Department of Electrical and Computer Engineering, National Technical University of Athens, 9 Iroon Polytexniou, 157 73 Athens, Greece

Received October 18, 2000; revised manuscript received July 9, 2001

The propagation of nonreturn-to-zero pulses, composed by a superposition of two exact shock-wave solutions of a complex-cubic Ginzburg–Landau equation linearly coupled to a linear nondispersive equation, is studied in detail. The model describes the distributed (average) propagation in a dual-core erbium-doped fiber-amplifier-supported optical-fiber system where stabilization is achieved by means of short segments of an extra lossy core that is parallel and coupled to the main one. The linear-stability analysis of the two asymptotic states of the shock wave in combination with direct numerical simulations provide necessary conditions for optimal propagation of the nonreturn-to-zero pulse. The enhancement of the propagation distance by at least an order of magnitude, under a suitable choice of the parameters, establishes the beneficial role of the passive channel.

OCIS codes: 060.2320, 060.2330, 060.2410, 060.5530, 190.4370, 190.5530.

1. INTRODUCTION

In the past few years there has been a considerable amount of theoretical research as well as experiments on designing long-haul and high-bit-rate fiber systems with periodic optical amplification for data transmission. Experiments performed as early as 1994 have demonstrated the potential of such a system, operating in the nonreturn-to-zero (NRZ) format for transoceanic optical communications.[1–3] Therefore the goal of achieving speed rates of 100 Gbits/s and over for distances exceeding 9000 km (transpacific order of magnitude) had been set as early as in the mid 1990s. Thus in the fall of 1996 the TPC-5CN, a 25 000-km transpacific optical cable loop linking Japan, Guam, Hawaii, and the United States was installed, operating at 5 Gbits/s per fiber. A few years later, the TPC-5CN was followed by the design of the more advanced TPC-6, which is a 20-channel (at 5 Gbits/s each) wavelength-division-multiplexed (WDM) NRZ system. Experiments demonstrated that WDM NRZ systems permitted transmission capacities of as much as 1 Tbit/s over 150 km[4] and 100 Gbits/s over 9100 km.[5] In such a system the limiting factors are the combined action of group-velocity dispersion (GVD), fiber nonlinearity [self-phase modulation (SPM)], and noise accumulation.

Numerical simulations were mainly employed for the evaluation of the role of these detrimental effects in the early stages of the research work.[6] The analytical descriptions were based on variational methods for obtaining the evolution of slowly varying parameters (such as the pulse width) of an ansatz of the shape of the pulse.[7,8] Analytical expression for the evolution of the guiding-center square pulse, under the influence of SPM and weak GVD, was also obtained by the WKB procedure on the nonlinear Schrödinger (NLS) equation in the normal dispersion regime.[9] Simple extension of the latter work (Ref. 9) to the hydrodynamic-type instabilities induced by cross-phase modulation and to the collisions in WDM NRZ transmissions based on coupled NLS equations has also been reported.[10] There is also an extension of the work in Ref. 9 to consider fast saturable absorption (nonlinear gain) simultaneously with GVD and SPM in a system with periodic amplification.[11]

It is common practice in the aforementioned systems that the losses, which are inevitably present in the fibers, are compensated by Er-doped fiber amplifiers.[12] The basis of the analytical investigation, on the other hand (model equation), is the aforementioned NLS equation, which supports soliton solutions (bright solitons) in the anomalous-dispersion regime.[13] However, optical amplifiers give rise to various instabilities and related detrimental effects, the most serious one being a random jitter of the solitons induced by their interaction with the optical noise generated by the amplifiers. A scheme that provides stabilization of the transmission of periodically amplified solitons is the use of guiding filters.[14,15] The model equation that takes into regard GVD, SPM, amplification, and fixed-frequency guiding filters is a modified NLS equation that is simultaneously a particular case of the complex-cubic Ginzburg–Landau (CCGL) equation,

$$iu_z + \left(\frac{D}{2} - i\right)u_{tt} + |u|^2u - iu = 0, \tag{1}$$

where z and t are the propagation distance and the so-called reduced time, and D is the dispersion coefficient. The SPM coefficient, excessive gain, and the effective filtering strength are all normalized to be unity. The gain and filtering terms in Eq. (1) are assumed to be uniformly distributed along the fiber communication link. This approximation, although it disregards the discrete character of the amplification and filtering, is well justified for suf-

ficiently broad solitons (with a temporal width of about or more than 10 ps), whose soliton period is sufficiently larger than the amplification spacing. A fundamental difference of the CCGL equation from the unperturbed NLS one is that, whereas the latter supports bright-soliton solutions (suitable for bit coding in telecommunication) only in the case of the anomalous-dispersion regime ($D > 0$), the former has exact bright solitary-wave solutions[16,17] in all cases. It also supports exact bright solitary-wave solutions in the case where the SPM coefficient is complex (if two-photon absorption effects are taken into account). Furthermore, CCGL supports exact dark solitary-wave solutions and, more importantly for the present work, shock-type solutions.[18,19]

Shock-type pulses could play the role of building blocks for NRZ pulses of arbitrary width: One may consider a NRZ pulse as a superposition of two shock-type pulses with a phase difference of π. However, the shock-type solutions of the model equation, Eq. (1), are extremely unstable since both the background and the cw are simultaneously unstable. Therefore apart from their mutual interaction, the shock-type constituents of NRZ pulse cannot propagate undistorted even for small distances. It is well known that the fundamental drawback of the model Eq. (1) is that is cannot support stable solutions, as the zero solution to this equation, i.e., the background, is unstable against perturbations $\sim\exp(-i\omega t)$ with $\omega^2 < 1$. This instability reflects a fundamental problem, which exists in systems in which the transmission of pulses is supported by means of a distributed linear gain. However, in the case of bright-soliton transmission, a new approach allowing one to suppress the instability of the background and thus open the way to the generation of absolutely stable bright solitons was recently proposed[20]: One should linearly couple the fiber to an additional lossy one. In this approach the active erbium-doped fiber-amplifier (EDFA) fiber segment inside the amplification hub is linearly coupled to an additional lossy fiber. This yields a system of two coupled CCGL equations that are then averaged over the amplification spatial period, rending a distributed model system. This model has also been numerically investigated[21] as well as fully analyzed for both time-domain-multiplexing (TDM) and WDM bright-soliton transmission systems.[22–24] It has been demonstrated that, in the new model's multidimensional parameter space, there is a vast region where the pulses are fully stable, for both the anomalous and the normal-dispersion regimes. Stable propagation for large distances (thousands of kilometers) for WDM and TDM systems has also been demonstrated. The aim of the present work is to investigate analytically and numerically the stability of the single shock-type solutions of Eqs. (2) and (3) as well as the stability of NRZ pulses formed by the superposition of such shock-type solutions. The stability regions for the zero state and the cw in the parameter space $\Gamma - K$ for both the anomalous and normal-dispersion regimes are obtained. The investigation extends to considering pairs of such NRZ pulses in a TDM system as well. In the latter case the relation between pulse width, temporal separation of pulses, and distance of stable (or almost stable) propagation is also numerically investigated. It will be shown that, although the zero state and the cw cannot be simultaneously stable, the presence of the passive channel highly increases the stable-propagation distance. Furthermore it will be shown that NRZ pulses in the normal-dispersion regime are characterized by much greater stable-propagation distances compared with the ones in the anomalous-dispersion regime. The latter are susceptible to strong broadening and distortion.

The proposed model is a distributed approximation (in the sense of a mean-field approach) for a transmission system with periodic optical amplifiers that are linearly coupled with lossy fibers in a dual-core (active EDFA–passive lossy) scheme within their respective amplification hubs. It can also model (with parameter values in a different range, of course) a dual-core long EDFA (of tens of kilometers) in a single point-to-point optical link.[25–27] From the mathematical point of view, the proposed model supports quite robust shock-type solutions and it is amenable to a far less tedious theoretical investigation as opposed to the realistic periodic-amplification system. From the practical point of view, these solutions can be equally considered as building blocks for NRZ pulses or temporal trains of NRZ pulses. The model provides the possibility of easily controlling the width and temporal separation of NRZ pulses. It can also be extended to WDM systems with distributed amplification as well as WDM transmission in optical links with periodically placed dual-core EDFAs. Extensive simulations of the latter and comparison with the distributed model is the subject of our current and future work.

The rest of the paper is organized as follows: In Section 2 we formulate the model, which describes the exact SW solutions of the Nozaki–Bekki type and how these solutions bifurcate with the trivial one. In Section 3 we perform a systematic linear-stability analysis of the zero and the continuous-wave (cw) solution in it, which provides a necessary basis for the direct numerical analysis of the shock-wave (SW) stability given in Section 4. The main differences between the modulational instability that the zero and the cw solutions exhibit in our case and the respective one for the NLS equation are also briefly discussed. In Section 4 we provide the conditions for maximizing the propagation distance of a SW solution and of an NRZ pulse formed by the combination of two exact SW solutions. The necessary connection with optical communications is also presented, by providing realistic values of the model in hand.

2. MODEL AND THE SHOCK-WAVE SOLUTIONS

The model is based on the following distributed system of equations:

$$iu_z + (D/2 - i)u_{tt} + |u|^2u - iu - iu = Kv, \quad (2)$$

$$i(v_z + cv_t) + (k_0 + i\Gamma)v = Ku. \quad (3)$$

Here u, v are the electric field of the two cores, K is the linear-coupling constant between the two cores, Γ models the losses of the passive core, and k_0 is the phase-velocity

mismatch between the two cores. Nonlinearity and dispersion in the passive core are assumed small compared with the loss coefficient.

This system of equations can also be derived in a systematic way for an optical link with periodically placed dual-core EDFAs by an averaging over the fast spatial scale, namely, the distance between two successive amplifiers. This mean-field approach is quite suitable in such cases since the length of a dual-core amplifier is much smaller than the spatial amplification period in all practical cases. It is straightforward, though tedious, to show that in the framework of this averaging, one needs only terms up to first and second order in the smallness parameter (namely, the ratio between the length of the EDFA and the spatial amplification period) for the active and the passive cores, respectively. Formally, the outcome of such an approach is again the system of Eqs. (2) and (3).

This system of equations possesses an exact analytical solution in the form originally found by Nozaki and Bekki[19] for the case of a single CCGL equation. With hyperbolic functions this analytical solution can be written, for the case of a dual-core fiber, as

$$u = u_0 \exp(ikz + i\theta\xi)(1 - \tanh\xi)(\operatorname{sech}\xi)^{i\mu}, \quad (4)$$

$$v = v_0 \exp(ikz + i\theta\xi)(1 - \tanh\xi)(\operatorname{sech}\xi)^{i\mu}, \quad (5)$$

where $\xi = \eta(t - cz)$. The relation providing the chirp parameter μ is

$$\mu = -3D/4 - (1/4)\sqrt{32 + 9D^2}, \quad (6)$$

and θ is related directly to the chirp through $\theta = 2/\mu$. The real amplitude u_0 and the complex amplitude v_0 in the gain and loss cores, respectively, are linearly related as $v_0 = (k_0 - k + i\Gamma)^{-1}Ku_0$. The wave number k is computed by the following third-order (in $\delta = -k + k_0$) algebraic equation:

$$\delta^3 + \left(\frac{Da_1}{a_2} - k_0\right)\delta^2 + (-K^2 + \Gamma^2)\delta + \Gamma(\Gamma - K^2)\frac{a_1}{a_2}D - k_0\Gamma^2 = 0, \quad (7)$$

where $a_1 = 5 + 9D^2/8$ and $a_2 = 8 + 9D^2/4$. For each acceptable wave number the parameter η, corresponding to the inverse value of the steepness of the shock, is given by

$$\eta^2 = \frac{[K^2\delta + k(\delta^2 + \Gamma^2)]Da_1 + (-K^2\Gamma + \delta^2 + \Gamma^2)a_2}{(\delta^2 + \Gamma^2)(D^2a_1^2 + a_2^2)}. \quad (8)$$

The amplitude of the solution u_0 is found to be proportional to η and is given by the relation

$$u_0^2 = -3\mu\eta^2\left(1 + \frac{D^2}{4}\right), \quad (9)$$

so that the expression u_0/η depends only on the dispersion parameter, D. Finally, the inverse propagation speed of the front is analogous to η, and more specifically

$$c = 6\eta\left(1 + \frac{D^2}{4}\right). \quad (10)$$

Equation (7) might provide one or three values for the wave number k that are real, a prerequisite for propagation. However, the physically acceptable ones must lead to positive values for u_0^2 or η^2 (since μ is always negative, these conditions are equivalent). Therefore the number of acceptable SW solutions might vary from one to three, and furthermore there is a region in the parameter space where, for all the available real values of the wave number (one or three), no solutions exist, i.e., $u_0^2 \leqslant 0$.

Varying the parameter values (the linear-coupling coefficient, K, for instance), physically acceptable solutions may either come into existence or cease to exist. Full representation of this process through respective bifurcation diagrams is a tedious and lengthy task. Without sacrificing generality and for the sake of clarity and economy of this paper, the investigation to be presented will be limited to the case where only one physically acceptable solution exits other than the zero solution. To compute the bifurcation point (zero-to-nonzero solution) one may obviously take advantage of the condition that near this point the amplitude of the SW is very small ($u_0^2 \ll 1$). Thus direct substitution of the ansatz (4) and (5) into Eqs. (2) and (3) yields the following algebraic relations:

$$-k - \theta\eta c + \left(\frac{D}{2} - i\right)[-\theta^2 - i(2\theta + \mu)]\eta^2 + u_0^2 - i - \frac{K^2}{-k + k_0 + i\Gamma} = 0, \quad (11)$$

$$i\eta c(1 + i\mu) + \left(\frac{D}{2} - i\right)[-1 - \theta\mu + i(\theta - \mu)]\eta^2 - 2u_0^2 = 0, \quad (12)$$

$$\eta^2(2 - \mu^2 + 3i\mu)\left(\frac{D}{2} - i\right) + u_0^2 = 0. \quad (13)$$

Assuming small-amplitude solutions $u_0 = \epsilon u^{(0)}$ and scaling the parameters as $k = k^{(0)} + \epsilon^2 k^{(2)}$, $\eta = \epsilon\eta^{(1)}$, $c = \epsilon c^{(1)}$, and $K = K^{(0)} + \epsilon^2 K^{(2)}$, one can obtain the values for the parameters of the SW near the bifurcation point. Specifically, to the zeroth order, the value of the wave number $k^{(0)}$ at that point is

$$k^{(0)} = \frac{k_0}{1 - \Gamma}, \quad (14)$$

which leads to $\delta = -k^{(0)} + k_0 = k_0\Gamma/(\Gamma - 1)$. The value of the coupling coefficient at the bifurcation point (to the zeroth order), on the other hand, can easily be expressed as a function of the losses in the passive core and also the phase-velocity mismatch, i.e.,

$$K^{(0)^2} = \Gamma\left[1 + \frac{k_0^2}{(\Gamma - 1)^2}\right]. \quad (15)$$

Equations (14) and (15) provide the relations between the parameters in Eqs. (2) and (3) at the bifurcation point.

Proceeding to the next order, it can be easily shown that the values of $u^{(1)}$, $c^{(1)}$, and $\eta^{(1)}$ are related exactly as in Eqs. (9) and (10), and the correction in the wave number is given by

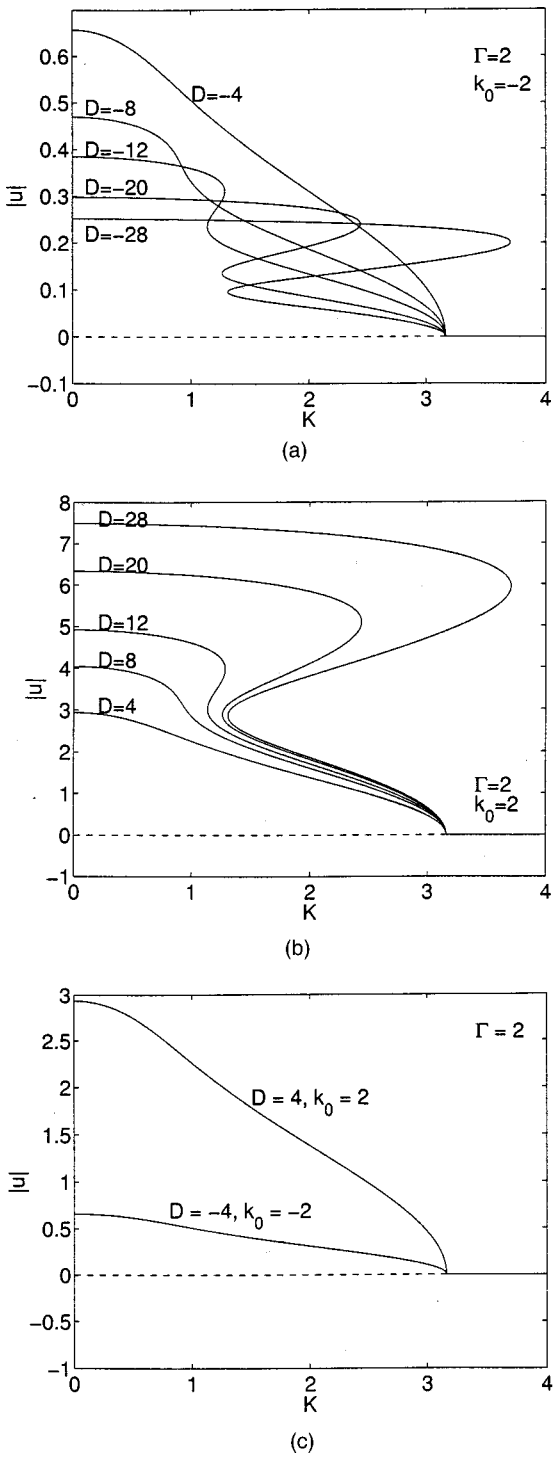

Fig. 1. Typical bifurcation diagram displaying the amplitude of the SW solution as a function of the coupling coefficient K for $|k_0| = 2$, $\Gamma = 4$, and for various values of (a) normal- and (b) anomalous-dispersion coefficient D. (c) Detail for $|D| = 4$, $|k_0| = 2$: The dashed (solid) curve part of the zero solution is unstable (stable) to zero-frequency perturbations. The nonzero solution is also depicted as a solid curve that consists of alternating stable and unstable parts.

$$k^{(2)} = \frac{\delta a_2 + \Gamma D a_1}{\Gamma - 1}\,\eta^{(1)^2}. \tag{16}$$

Finally, the approximate (to first order) squared inverse slope is proportional to the variation in the coupling coefficient,

$$\eta^{(1)^2} = -\frac{2K^{(0)}K^{(2)}}{k_0(\Gamma + 1)(\delta a_2 + \Gamma D a_1)/(\Gamma - 1)^2 + \Gamma a_2 - \delta D a_2} = \sigma K^{(2)}. \tag{17}$$

For $\sigma > 0$ ($\sigma < 0$) a SW solution near the bifurcation point emerges if $K^{(2)} < 0 (K^{(2)} > 0)$. The amplitude of the bifurcation can be easily obtained by utilizing Eqs. (9) and (17). In Fig. 1, typical bifurcation diagrams are shown where the amplitude of the SW is plotted as a function of the coupling coefficient, K, in a case where $\Gamma = 2$. In Figs. 1(a) and 1(b), various cases for normal (with $k_0 = -2$) and anomalous dispersion (with $k_0 = 2$) are respectively shown, and a single-case comparison (with $|D| = 4$) is shown in Fig. 1(c). Notice that the bifurcation point depends on the absolute value of the phase-velocity mismatch, k_0, as Eq. (15) also suggests. The dashed (solid) curve part of the zero solution is always unstable (stable) to zero-frequency perturbations, as is discussed in Section 3. A solid curve also depicts the nonzero SW solution and consists of parts of alternating character (stable–unstable to zero-frequency perturbations).

3. LINEAR STABILITY OF THE SOLUTIONS

The SW solution reaches asymptotically two different states at $\xi \to \pm\infty$. Specifically at $\xi \to \infty$ it reaches the zero solution, and at $\xi \to -\infty$ it reaches the corresponding continuous-wave (cw) solution. The stability of the SW is related to the stability of its asymptotic states, i.e., the stability of the zero solution and the stability of the respective cw solution.

Proceeding to the stability analysis of the zero solution, we first notice that in the case of a single CCGL equation the background is unstable for all the frequencies that satisfy the condition $\omega^2 < 1$ and stable for all other frequencies. The instability mechanism can be understood as follows: The gain term, $-iu$, causes exponential growth that can be matched only by the losses the diffusion term (filtering), iu_{tt}, is responsible for. The latter becomes important at high frequencies (where the second time derivative of the solution becomes important). Similarly, the energy associated with the high-frequency part of the instability spectrum can be dissipated by the filtering losses. However, this energy dissipation cannot efficiently suppress the low-frequency part of the instability spectrum. The dual-core model[20] provides that extra mechanism (through energy deposition in the lossy core) necessary for the complete suppression of these low-frequency instabilities.

The stability of the physically acceptable SW solutions is tightly connected with the stability of the zero background and the stability of the asymptotic nonzero state (cw solution). In order to investigate the stability of the

former, Eqs. (2) and (3) are linearized by considering the following small amplitude fluctuations of the zero background:

$$u = u_1 \exp[i(kz - \omega t)], \quad v = v_1 \exp[i(kz - \omega t)]. \tag{18}$$

Here k and ω are respectively the wave number (generally, complex) and the frequency (always real) of the fluctuations. Then the stability region in the plane of the model's parameters (Γ, K, k_0, c) is determined by the condition $\mathrm{Im}\, k > 0$, which, after some algebra, yields the following inequality:

$$K^2 - \Gamma(1 - \omega^2)\left[1 + \frac{(k_0 + c\omega + D\omega^2/2)^2}{(\Gamma - 1 + \omega^2)^2}\right] > 0. \tag{19}$$

This inequality holds automatically, provided that $\omega^2 > 1$, which is the aforementioned stability relation for the single CCGL equation. Therefore one needs to consider Eq. (19) only for $\omega^2 < 1$. Additionally, it is readily seen that the condition $\Gamma > 1$ must hold for the left-hand side of Eq. (19) to remain finite at these values of ω. In the case $\omega^2 < 1$, Eq. (19) can be simplified in some special cases, e.g., $k_0 = 0$, $c = 0$, $D = 0$, or $\Gamma \gg 1$, or $k_0 = 0$, $\omega = 0$, yielding $1 < \Gamma < K^2$, which is a well-known necessary condition found in the recent scientific literature.[20,21,28]

However, extensive numerical investigation shows that the condition of stability of the zero solution, inequality (19), over the entire perturbation holds for the frequency spectrum for parameter values (K, Γ, k_0, c, and D) that are outside the region of the existence of the nonzero solution [i.e., real wave number k and amplitude u_0 values in Eq. (4)]. Nevertheless, physically acceptable nonzero solutions may exist for parameter values for which the zero solution is only partially stable (not for all ω values). Specifically, one may focus on the bifurcation process as shown in Fig. 1(c): It is generally true that at the bifurcation point, Eqs. (9) and (10) imply that $c = 0$. Setting $\omega = 0$ to Eq. (19), one obtains an inequality that states that the minimum acceptable value of the linear-coupling coefficient for stability to perturbations with $\omega = 0$ is given by Eq. (15). That is, the minimum value is precisely the bifurcation value of the coupling coefficient. Thus the nonzero SW solution bifurcates from the zero solution at the point where the latter becomes unstable at zero frequency. Therefore the stability in the vicinity of the latter will play an important role in the rest of the investigation.

On the other hand, the cw solution obtained from Eqs. (4) and (5) must also be stable. Taking the limit $\xi \to -\infty$ in Eqs. (4) and (5) and neglecting a constant phase term yields

$$\{u, v\} = \{U_0, V_0\}\exp[i(\kappa z - \omega t)], \tag{20}$$

where $\{U_0, V_0\} = 2\{u_0, v_0\}$, $\kappa = k - (\theta + 1)\mu\eta c$, and $\omega = -(\theta + 1)\mu\eta$. By imposing the conditions given by Eqs. (6)–(10) this cw represents the asymptotic state of the SW solution (4) and (5). To investigate the stability of the cw solution, Eq. (20) is perturbed by substituting into Eqs. (2) and (3) the following expressions:

$$u = (U_0 + \epsilon U_1)\exp[i(\kappa z - \omega t)],$$

$$v = (V_0 + \epsilon V_1)\exp[i(\kappa z - \omega t)],$$

with ϵ being a small parameter. To order ϵ, the linearized system is

$$\left[-\kappa - \omega^2\left(\frac{D}{2} - i\right) + 2U_0^2 - I\right]U_1 + U_0^2 U_1^* + \left(\frac{D}{2} - i\right) \times (-2i\omega U_{1t} + U_{1tt}) + iU_{1z} - KV_1 = 0,$$

$$(-\kappa + k_0 + i\Gamma)V_1 + iV_{1z} - KU_1 = 0.$$

By separating the real and the imaginary parts of these equations, that is, $U_1 = U_1^{(r)} + iU_1^{(i)}$, $V_1 = V_1^{(r)} + iV_1^{(i)}$, one obtains four real differential equations for these terms. Expressing the latter as $\{U_1^{(r)}, U_1^{(i)}, V_1^{(r)}, V_1^{(i)}\} = \{U^{(r)}, U^{(i)}, V^{(r)}, V^{(i)}\}\exp[i(Qz - \Omega t)]$ + c.c. (c.c. denotes complex conjugation), the dispersion relation between the wave number Q and the frequency of the perturbation Ω is obtained as a solution of the quintic equation

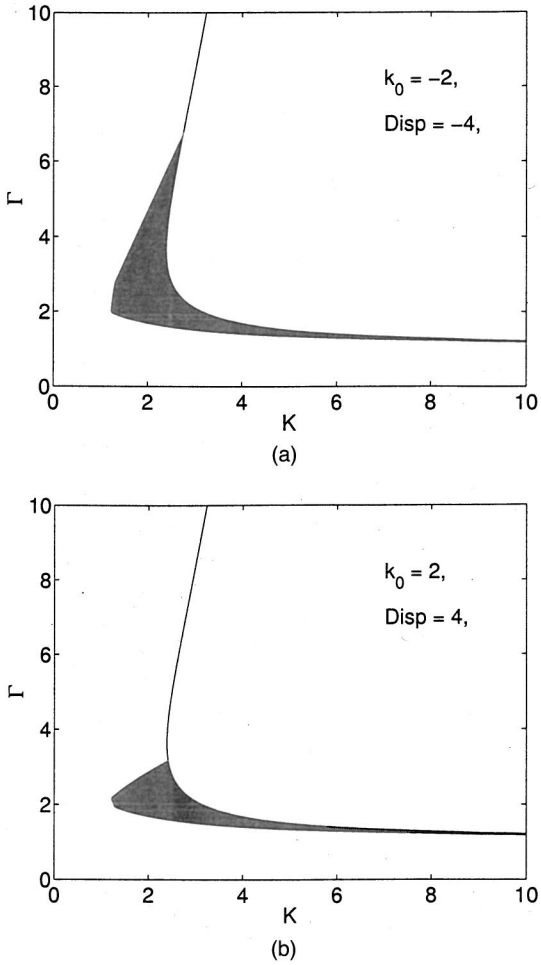

Fig. 2. Region of stability of the cw solution at the zero-frequency (shaded region) and the solid curve on the right separating the region of existence of SW solutions in the (Γ, K) parameter plane (a) for $k_0 = -2$, $D = -4$ and (b) for $k_0 = 2$, $D = 4$.

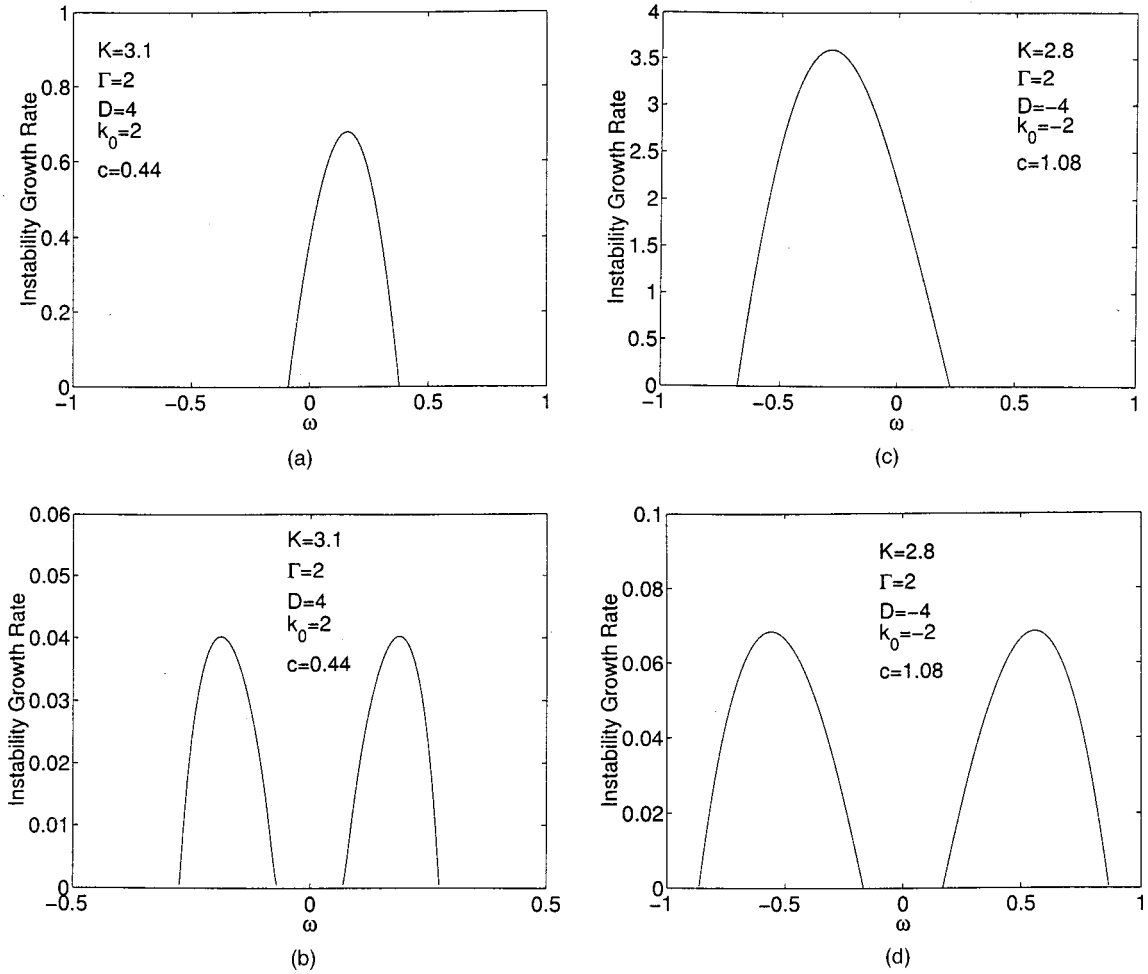

Fig. 3. Instability growth rates as functions of the frequency for (a)–(c) the zero solution and for (b)–(d) the cw solution with (a), (b) $k_0 = 2, D = 4,\ c = 0.44, K = 3.1$ and (c)–(d) $k_0 = -2, D = -4,\ c = 1.08, K = 2.8$. The value of Γ is 2.

$$Q^4 + 2i(B - \Lambda)Q^3 + (-AA' - B^2 - \Lambda^2 + 4B\Lambda - \Delta^2 - 2K^2)Q^2 + 2i[K^2(\Lambda - B) + AA'\Lambda - B\Delta^2 + B\Lambda(B - \Lambda)]Q - 2BK^2\Lambda - (A + A')K^2\Delta + B^2(\Lambda^2 + \Delta^2) + AA'(\Lambda^2 + \Delta^2) + K^4 = 0, \quad (21)$$

where

$$A = -k - D(\omega + \Omega^2)/2 + U_0^2 + 2i\Omega\omega,$$

$$A' = -k - D(\omega + \Omega^2)/2 + 3U_0^2 + 2i\Omega\omega,$$

$$B = 1 - (\omega^2 + \Omega^2) - iD\omega\Omega,$$

$$\Lambda = \Gamma - ic\Omega,$$

$$\Delta = -k + k_0 + c\omega.$$

The cw solution will be stable in the case where all four values of the wave number Q obtained from the quintic Eq. (21) will have their imaginary parts greater than or equal to zero, i.e., $\mathrm{Im}\, Q_i > 0\ i = 1..4$. The complexity of Eq. (21) is a serious obstacle for further analytical calculations. Therefore what follows is purely a result of extensive numerical investigation.

Solving Eq. (21) numerically in the four-dimensional parametric space K, Γ, D, k_0, no region of full stability (stability for all frequencies of the perturbation) is found. Nevertheless, one can find isolated regions where the cw solution is stable for the zero frequency, $\Omega = 0$. The zero-frequency perturbations are generally considered as the "most dangerous" perturbations, since when they turn unstable, they affect the asymptotic state not locally in time but as a whole. Temporally localized unstable perturbations, on the other hand, pose a much less detrimental effect that might remain confined for long propagation distances before it distorts or completely destroys the initial (at $z = 0$) waveform (the SW in the case in hand). Therefore it is inside the regions of stability at $\Omega = 0$ where one expects maximum propagation distance for a single SW. According to the numerical investigations made, such regions exist only for the cases where the normalized phase-velocity mismatch between the active and the passive cores, k_0, and the normalized dispersion coefficient in the active core, D, have the same sign. In the cases where the dispersion coefficient is zero, no such regions were found. In Figs. 2(a) and 2(b) two such examples corresponding to the anomalous and normal-dispersion regimes respectively are shown. As one can

see, the regions where the cw is stable to the aforementioned zero-frequency perturbations are bounded by the curves that limit the existence of the SW solutions.

In Figs. 3(a)–3(c) and Figs. 3(b)–3(d) the instability growth rates of the zero and the cw solutions are shown respectively as functions of the perturbation frequency. Both cases of the anomalous [$D = 4$, $k_0 = 2$, $K = 3.1$, and $c = 0.44$ in Figs. 3(a)–3(b)] and the normal [$D = -4$, $k_0 = -2$, $K = 2.8$, and $c = 1.08$ in Figs. 3(c)–3(d)] dispersion are considered. The value of the normalized loss rate in the respective passive cores, Γ, is 2 for both cases. In both anomalous and normal cases the parameters chosen correspond to points inside the cw stability regions displayed in Figs. 2(a) and 2(b), respectively. In Figs. 3(a)–3(c) the instability growth rate of the zero solution corresponds to the inverse negative part of the left-hand side of Eq. (19). In Figs. 3(b)–3(d), on the other hand, the respective instability growth rates correspond to the inverse of the negative imaginary parts that two (out of four) eigenvalues possess [obtained from Eq. (21)]. The other two of the eigenvalues are fully stable (possessing positive imaginary parts). One can easily observe that the two sidebands of the cw instability are located near the zero perturbation frequency, while there is, as expected, a region of stability in the neighborhood of the zero frequency. However, as already discussed, both the zero and the cw solutions cannot be simultaneously stable to zero-frequency perturbations, a fact that is perfectly clear from these figures.

It is worth mentioning that the aforementioned modulational instability is quite different than the one the usual NLS equation exhibits: It is well known, theoretically and experimentally,[29,30] that a cw in the NLS equation and in the anomalous-dispersion regime is unstable to small modulations in amplitude, and the instability eventually evolves to a short pulse train. On the other hand, in the normal-dispersion regime, the same equation supports dark-soliton solutions whose cw asymptotic states are modulationally stable. In contrast, as we have seen, the system in hand possesses a much richer behavior as far as the zero and the cw solutions are concerned, depending upon the choice of the parameters involved. Furthermore, a model based on the NLS equation is energy conserving, thus leading, upon modulation, to the formation of structures that conserve the overall energy, whereas the model based on the CCGL equation, as the one in hand, is dissipative and therefore possibly leading to chaotic behavior in certain cases.

4. LAMINAR PROPAGATION FOR SINGLE SHOCK WAVES AND NONRETURN-TO-ZERO COMBINATIONS

Initially the propagation of a single exact SW solution is examined, and the role of the coupling coefficient, K, between the two cores is quantitatively investigated. It is expected that by increasing the coupling coefficient, the maximum propagation distance before the instability, which in both the zero background and the cw asymptotic state come into play, will also be increased. This propagation distance will be called "*laminar*" in the rest of the paper. Both cases of anomalous and normal dispersion are considered. In each of these cases the phase-velocity mismatch between the active and the passive cores is chosen to satisfy the condition $k_0 D > 0$. It is specifically set as $|k_0| = 2$, since large values of $|k_0|$ increase the instability of the zero solution: The region of values of the physical parameters that can satisfy inequality (19) is considerably reduced as $|k_0|$ increases. Thus both the instability bandwidth and the instability growth rate of the zero solution is increased. It is also set as $\Gamma = 2$ in order to ensure that the corresponding cw solution will lie in its respective stability region.

In Fig. 4 a single shock propagating laminarly for considerable distance is shown. Here the parameter values refer to a normal-dispersion case, namely, $D = -4$, $k_0 = -2$, $K = 2.8$, $\Gamma = 2$, and $c = 1.08$. In Fig. 5 the laminar-propagation distance as a function of the coupling coefficient K is displayed in the cases $D = 4$ (crosses) and $D = -4$ (stars). As it is readily seen, the laminar-propagation distance increases with K. Thus larger values of laminar-propagation distance (at least an order of magnitude) can be achieved for moderate values of the coupling coefficient, K, as compared with the laminar-propagation distance without the passive core present ($K = 0$).

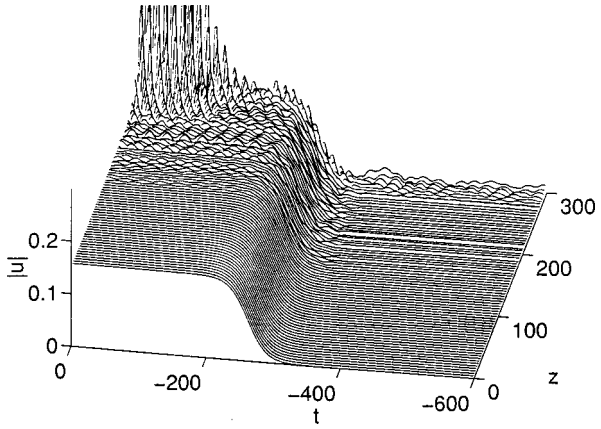

Fig. 4. Single shock propagating laminarly ending with onset of blowup. Here, $D = -4$, $k_0 = -2$, $K = 2.8$, $\Gamma = 2$, and $c = 1.08$.

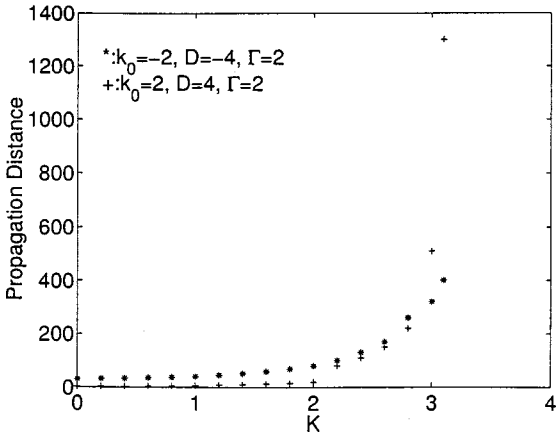

Fig. 5. Laminar-propagation distance as a function of the coupling coefficient K for $D = 4$, $k_0 = 2$ (crosses) and for $D = -4$, $k_0 = -2$ (stars).

As it is already pointed out, the construction of a temporally localized pulse, perhaps as bound states of two interacting SWs, is very important for optical communications. A NRZ pulse can be modeled at $z = 0$ as a superposition of two (eventually interacting as they propagate) exact SWs. These two SW constituents are acceptable as long as the physical parameters of the system lead to stable cw (common) solutions to zero-frequency perturbations. This superposition can be written in the following general form:

$$u = u_0 \exp(ikz)\{\exp[i\theta\eta(xi - \tau/2)][1 - \tanh \eta(\xi - \tau/2)][\operatorname{sech} \eta(\xi - \tau/2)]^{i\mu} - \exp(i\theta\xi_2)[1 - \tanh \eta(\xi + \tau/2)][\operatorname{sech} \eta(\xi + \tau/2)]^{i\mu}\exp(-i\phi)\}, \quad (22)$$

where $\xi = t - cz$, τ is the temporal separation between the two shocks, and ϕ is the phase mismatch between them. To generate a localized pulse, Eq. (22) must reach asymptotically the zero solution as $\xi \to \pm\infty$. This condition is always satisfied for $\xi \to \infty$, but for $\xi \to -\infty$ the condition is fulfilled when the two cw solutions have a phase difference of a multiple of 2π. This condition leads to a certain relation between τ and ϕ as

$$\tau = \frac{2\pi N + \phi}{\eta(\theta + \mu)}, \quad (23)$$

where N is an integer. Notice that without loss of generality one can assume that $N = 0$. The pulse width $\eta\tau$ can be easily controlled in terms of the phase difference ϕ. This is a major advantage of this SW-based NRZ propagation: In contrast, in the case of bright-soliton propagation in similar dual-core systems,[16,17] there is more freedom in selecting pulse characteristics (the pulse width, for instance, becomes a free parameter), whereas all the parameters of the chirped bright-soliton pulse are determined explicitly from the parameters of Eqs. (2) and (3).

The value of the chirp in the SW constituents of the NRZ pulse characterizes the interaction: It is strong (weak) if $\mu \gg 1$ ($\mu \ll 1$). In the case of strong interaction, fluctuations in the initial pulse profile will be developed near $\xi + \tau/2 = 0$. The analytical form of these fluctuations can be obtained assuming that $\eta\tau \gg t - cz$, so that the magnitude of Eq. (22) can be well approximated by

$$|u|^2 = 4u_0^2\left\{\left(\frac{1 + \tanh \xi}{2}\right)^2 + 2(1 - \tanh \xi)\sin^2\left[\frac{\mu}{2}\ln\left(\frac{\operatorname{sech} \xi}{2e^{\xi}}\right)\right]\right\}. \quad (24)$$

Equations (6)–(24) suggest that for large positive values of D (anomalous-dispersion regime) corresponding to $\mu \gg 1$, the second oscillating term on the right-hand side of Eq. (24) becomes important, and the interaction is therefore strong. On the other hand, for large negative values of D (normal-dispersion regime), the oscillating term is small compared with the first term, and the interaction is weak.

Let us consider an initial condition ($z = 0$) given by Eq. (22) that propagates according to the model, Eqs. (2) and (3). The propagation of such an initial condition is, as already mentioned, highly affected by the value of the chirp μ. The laminar-propagation distance is controlled by the regions of instability growth rates for both the zero background and the cw asymptotic state. The values of the parameters Γ, K, and k_0 must be properly chosen to maximize this laminar-propagation distance. A strategy could be fixing the parameters in such a way that the respective cw asymptotic state (the plateau of the NRZ pulse, in other words) is stable to the zero-frequency perturbations.

A typical example for the anomalous-dispersion case with $D = 4$, $k_0 = 2$, and $K = 2.8$ (strong-interaction regime) shown in Fig. 6(a) is contrasted with an example for the normal-dispersion regime with $D = -4$, $k_0 = -2$, and $K = 2.8$ (weak-interaction regime) shown in Fig. 6(b). The value of Γ in Fig. 6 is 2. In the first case the initial pulse profile oscillates near $\xi + \tau/2 = 0$ and the initial pulse width tends to increase linearly with the propagation distance z. Specifically, the constituent SW with temporal location $\xi - \tau/2 = 0$ propagates with the same speed as expected by the exact SW solution [Eq. (10)], whereas the second constituent located at $\xi + \tau/2 = 0$ propagates with a smaller speed. This results in a broadening of the pulse. Furthermore, the amplitude of the cw near the temporal location $\xi - \tau/2 = 0$ remains constant with z, and near $\xi + \tau/2 = 0$ a region is generated where the amplitude varies rapidly between arbitrary values located mainly in the range between zero and two times the initial cw amplitude. This disturbance tends to spread out but does not destroy the pulse. This result can be viewed as a consequence of the cw stability of the zero frequency. The pulse blows up when the zero-solution instability sets in. In the second case, the initial pulse profile stays smooth over the laminar-propagation distance due to the low value of the chirp the constituent SW solutions possess. After this distance, the chirp causes the instability of the cw to set in. Then the instability grows rapidly and finally tends to radiate from the pulse.

Different initial pulse profiles have also been tested. Of particular interest is the generation of a NRZ pulse by superimposing an exact shock-wave solution and another chirpless SW, that is, without the $[\operatorname{sech}(\xi + \tau/2)]^{i\mu}$ term. As already mentioned, this term is responsible for the strong oscillations and lack of any laminar propagation of the initial pulse profile in the strong-interaction regime. Numerical simulations performed for this type of an initial condition lead to the conclusion that these short NRZ pulses exhibit very similar behavior to those composed of two exact (chirped) single shocks: The evolution of the initial pulse profile is quite similar to that of the laminar propagation, for both the anomalous- and normal-dispersion regimes. A quite interesting behavior exists for cases where the shock-wave constituents of the NRZ pulse are initially ($z = 0$) chirpless: In the anomalous-dispersion regime there is a moderate broadening of the NRZ pulse, [Fig. 6(c)]. The amplitude, however, lacks any erratic behavior [as compared with Fig. 6(a)], although there is a smooth and rather slow amplitude oscillation. In the normal-dispersion regime [Fig. 6(d)], on

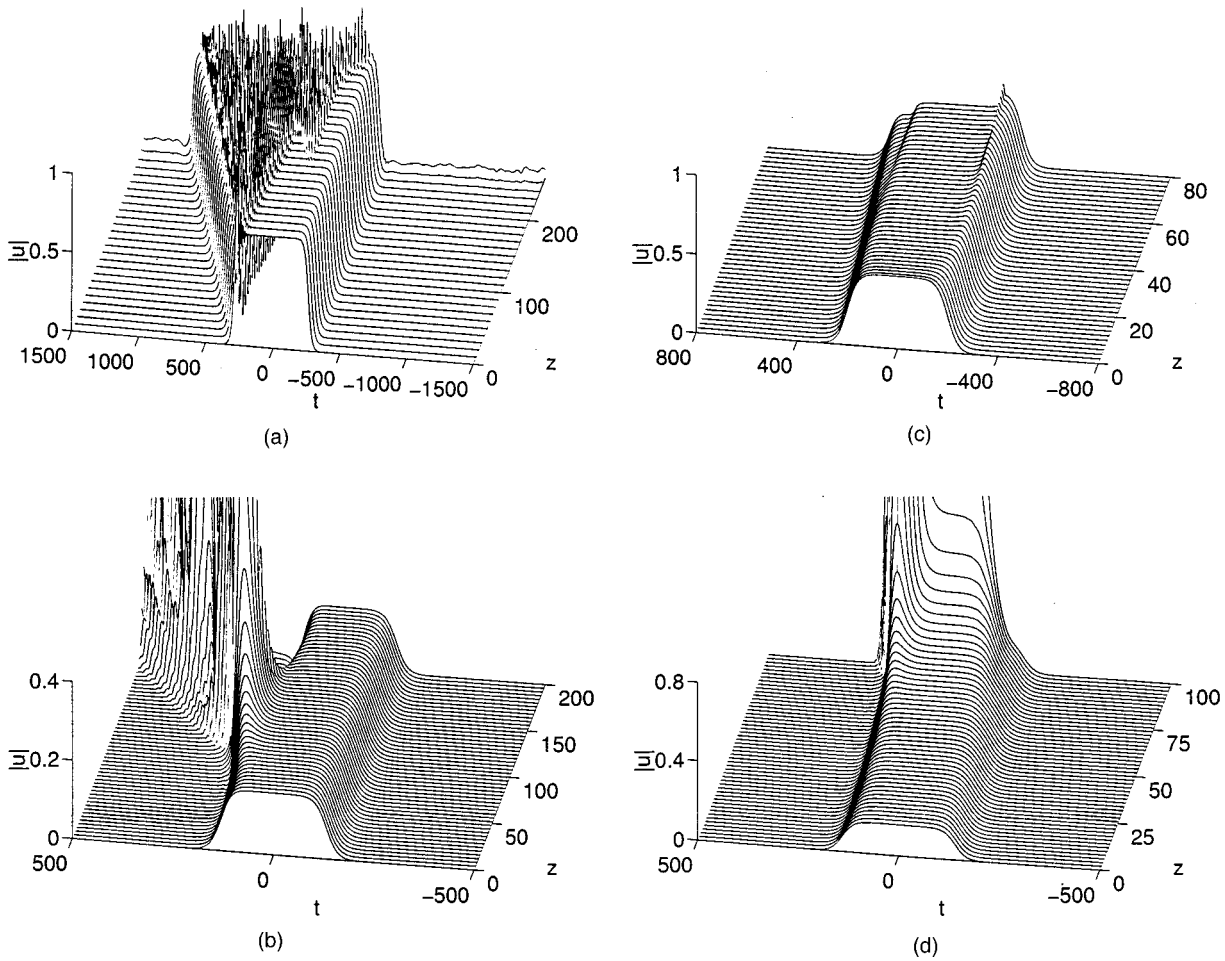

Fig. 6. Typical examples for NRZ pulse propagation: (a)–(c) anomalous-dispersion regime with $D = 4$, $k_0 = 2$, and (a) $K = 2.8$, (c) $K = 3$; (b)–(d) normal-dispersion regime with $D = -4$, $k_0 = -2$, $K = 2.8$. (a), (b) The NRZ pulse consists of two exact shock-wave solutions; the (c)–(d) NRZ pulse consists of two initially unchirped shock-wave solutions. The value of Γ is 2.

the other hand, the pulse is more unstable than the prior case. This leads to a blowup of the NRZ pulse although the pulse width behaves reasonably well.

In Fig. 7(a) the laminar-propagation distance of an initial pulse profile in the form of Eq. (22) is displayed as a function of the coupling coefficient K for two values of the dispersion located in the normal-dispersion regime, namely, $D = -4, -8$. The values of the rest of the parameters are $\Gamma = 2$ and $k_0 = -2$. As the coupling between the two cores is increased, the propagation distance of the pulse is highly increased. Also the enhancement of the absolute value of the dispersion tends to increase the propagation distance. This can easily be explained by the fact that the larger the value of $-D$ is, the smaller the value of μ will be [as given by Eq. (6)], and the interaction between the two SWs will become weaker. However, there is a trade-off in the choice of D: It is clear from the bifurcation diagram, Fig. 7(b), that the larger the value of $-D$ is, the smaller the amplitude of the NRZ pulse becomes.

The major advantage of using SWs as building blocks of NRZ pulses is the ability to control the width of the pulse. This leads to the ability of using pulses of variable width in an NRZ communication system. In a bit-transmission system that uses the NRZ format for the pulse that encodes "1," two successive "1's" (i.e., two successive pulses) are realized as a single NRZ pulse twice as broad. As observed by numerical simulations, for narrow pulses, i.e., when the temporal separation τ is small (then the NRZ pulse resembles a bright pulse), the laminar-propagation distance scales with τ. However, when an NRZ pulse is well formed, the propagation distance becomes insensitive to τ. Therefore there is an abundance of NRZ pulses of different pulse widths (encoding a variety of strings of bits) that can laminarly propagate for long distances in the normal-dispersion regime. Such a typical example can be seen in Fig. 8 for the case $D = -4$, $k_0 = -2$, $K = 2.8$, and $\Gamma = 2$.

The applicability of the model in hand to optical communication systems can be illustrated by the following example: As already mentioned, Eqs. (2) and (3) describe the average soliton profile propagating in an optical fiber.[13] A necessary condition for lossless evolution is given by $z_a \gamma = L_a g_0$, where z_a is the spatial period in a periodic amplification scheme and L_a is the amplifier (EDFA) length. Here, γ describes the line fiber loss and g_0 is the gain of the EDFA. For a single-mode and dispersion-shifted fiber, losses are minimal at the wavelength $\lambda = 1.55\,\mu$m, where $\gamma = 0.2$ dB/km $\approx 0.05\,\text{km}^{-1}$. Also typical values for the amplifier spacing and the am-

plifier length are given by $z_a = 40\,\mathrm{km}$ and $L_a = 40\,\mathrm{m}$, so that from the previously mentioned condition the amplifier gain must have the value $g_0 = 0.2\,\mathrm{dB/m} \approx 50\,\mathrm{km}^{-1}$

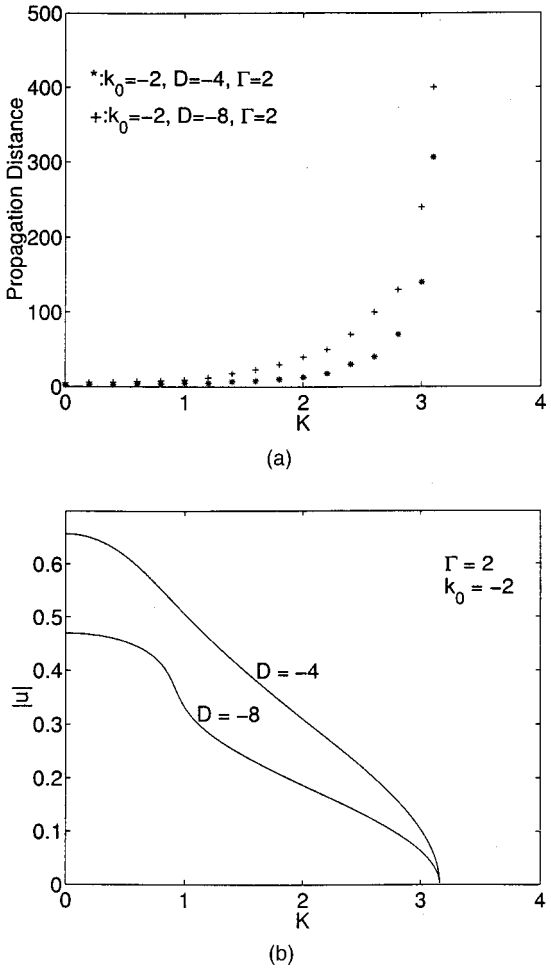

Fig. 7. (a) Laminar-propagation distance as a function of the coupling coefficient K for $D = -4$ and $D = -8$. (b) The respective bifurcation diagram for the two cases in (a) displaying the amplitude of the SW solution as a function of the coupling coefficient K. The values of the rest of the parameters are $\Gamma = 2$ and $k_0 = -2$.

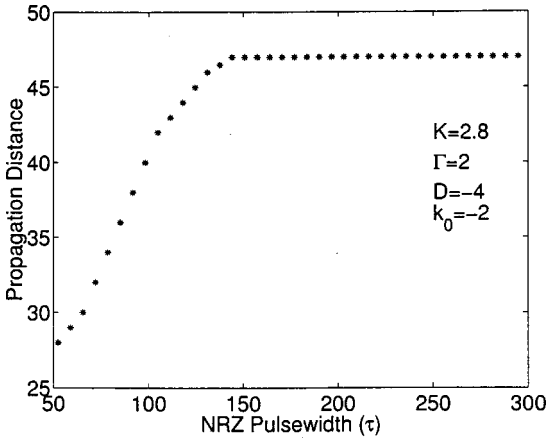

Fig. 8. Laminar-propagation distance of an NRZ pulse as a function of the temporal pulse width, τ, for the case $D = -4$, $k_0 = -2$, $K = 2.8$, and $\Gamma = 2$.

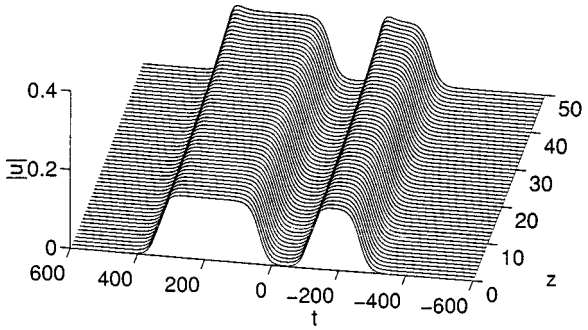

Fig. 9. Propagation of two pulses representing four successive bits of information (1101) for $D = -4$, $k_0 = -2$, $K = 2.8$, and $\Gamma = 2$. The full width at half-maximum (FWHM) of the pulses is 32 ps, and the temporal separation between them is ~60 ps.

in order to overcome the losses of the fiber. In Fig. 8 the values of the parameters for optimal propagation (i.e., the minimum pulse width obtaining maximum propagation distance) are $\tau = 140$ and a normalized propagation distance of ~50. In our model, time and distance are normalized to the values $\tau_0 = (\gamma_2/g)^{1/2}$ and $z_0 = 1/g$, respectively. Here g is the distributed energy excess needed to overcome both the losses due to the filtering and the losses in the passive core, whereas γ_2 represents the distributed action of the bandpass filter. Finally, the dispersion parameter is obtained from the relation $\beta_2 = D\gamma_2$. Assuming typical values $\gamma_2 = 0.005\,\mathrm{ps}^2/\mathrm{km}$ and $g = 0.005\,\mathrm{km}^{-1}$, we obtain $\tau_0 = 1\,\mathrm{ps}$ and $z_0 = 200\,\mathrm{km}$. For the case represented in Fig. 8 (corresponding to $K = 2.8$, $\Gamma = 2$, $D = -4$, and $k_0 = -2$), the optimal value of the temporal separation between two successive bits of information is $T = 150\,\mathrm{ps}$, and the laminar-propagation distance is $L \approx 10\,000\,\mathrm{km}$. In another typical example (for the same values of the parameters) we choose $\gamma_2 = 0.005\,\mathrm{ps}^2/\mathrm{km}$ and $g = 0.03\,\mathrm{km}^{-1}$, resulting in $T = 56\,\mathrm{ps}$ and $L = 1600\,\mathrm{km}$. In Fig. 9 the interaction of two such pulses representing four successive bits of information (1101) is displayed. Here the parameters of Eqs. (2) and (3) are also set to the values $K = 2.8$, $\Gamma = 2$, $D = -4$, and $k_0 = -2$. The respective pulse widths for the first (11) and the second segment (1) are 300 ps and 150 ps, and the intermediate bit 0 also has a pulse width of 150 ps. The laminar-propagation distance is $L \approx 10\,000\,\mathrm{km}(50z_0)$. It is evident that the laminar-propagation distance of this bit segment is determined almost exclusively by the propagation distance of a single NRZ pulse.

5. CONCLUSION

In this work we explore the possibility of stabilizing NRZ pulses in optical communication systems with periodic use of EDFAs. The stabilization of the pulses is achieved by means of sort segments of an extra lossy core, which is parallel coupled to the EDFA. The model in hand constitutes two coupled CCGL equations for the respective active (EDFA) and passive (lossy) cores and represents a distributed picture (averaged over the spatial amplification period) of the optical link. Nevertheless, it models

equally well a dual-core long EDFA point-to-point optical link with the second core being a common-type lossy one. The beneficial role of the passive channel is well established by the fact that the laminar-propagation distance is highly increased (at least an order of magnitude) with a suitable choice of the parameters. Thus our model in hand provides an attractive way for the optimal use of EDFAs with NRZ signal formats.

The NRZ pulse can be considered as being formed by the interaction of two exact SW solutions of the system of equations the model is based on with a phase difference of π. Optimal values for the parameters were obtained to achieve maximum propagation distance. It was found that simultaneous stabilization of the zero solution and the corresponding cw solution cannot be achieved. However, one may easily choose the parameters of the media (active, passive) in such a way that the instability growth rate becomes minimal. Furthermore, the chirp that is responsible for the deconstruction of the pulse may similarly be reduced.

Propagation of NRZ pulses has been tested for both signs of the dispersion. In the anomalous-dispersion regime the chirp parameter is big enough to immediately generate various detrimental effects. However, if the NRZ shock-wave constituents are initially ($z = 0$) unchirped, the NRZ exhibits only moderate pulse-width broadening and amplitude oscillations over reasonably long laminar-propagation distances. In contrast, in the normal-dispersion regime (corresponding to small values of the chirp), the NRZ pulse achieves high laminar-propagation distances in the case where the NRZ pulse consist of two exact (i.e., chirped) solutions. In conclusion, the normal-dispersion regime is more favorable for undistorted NRZ pulse propagation.

ACKNOWLEDGMENTS

The authors are indebted to B. A. Malomed and D. J. Frantzeskakis for useful discussions. This work has been supported in part by the Archimedes Grant of the Institute of Communications and Computer Systems/National Technical University of Athens and in part by the General Secretariat of Research and Development under Contract PENED-95/644.

REFERENCES

1. N. S. Bergano, C. R. Davidson, G. M. Homsey, D. J. Kalmus, P. R. Trischitta, J. Aspell, D. A. Gray, R. L. Maybach, S. Yamamoto, H. Taga, N. Edagawa, Y. Yoshida, Y. Horiuchi, T. Kawazawa, Y. Namihira, and S. Akiba, "9000 km, 5 Gb/s NRZ transmission experiment using 274 erbium-doped fiber amplifiers," in *Optical Amplifiers and Their Applications*, Vol. 14 of 1994 OSA Technical Digest Series (Optical Society of America, Washington D.C., 1994), paper PD7.
2. H. Taga, N. Edagawa, S. Yamamoto, and S. Akiba, "Recent progress in amplified undersea systems," J. Lightwave Technol. **13**, 829–834 (1995).
3. N. S. Bergano and C. R. Davidson, "Circulating loop transmission experiments for the study of long-haul transmission systems using erbium-doped fiber amplifiers," J. Lightwave Technol. **13**, 879–889 (1995).
4. H. Onaka, H. Miyata, G. Ishikawa, K. Otsuka, H. Ooi, Y. Kai, S. Kinoshita, M. Seino, H. Nishimoto, and T. Chikama, in *Optical Amplifiers and Their Applications*, Vol. 2 of 1996 OSA Technical Digest Series (Optical Society of America, Washington D.C., 1996), paper PD19.
5. N. S. Bergano, C. R. Davidson, D. L. Wilson, F. W. Kerfoot, M. D. Trembay, M. D. Levonas, J. P. Morreale, J. D. Evankow, P. C. Corbett, M. A. Mills, G. A. Ferguson, A. M. Vengsarkar, J. R. Pedrazzani, J. A. Nagel, J. L. Zyskind, and J. W. Sulhoff, in *Optical Amplifiers and Their Applications*, Vol. 2 of 1996 OSA Technical Digest Series (Optical Society of America, Washington D.C., 1996), paper PD23.
6. D. Marcuse, A. R. Chraplyvy, and R. W. Tkach, "Effect of fiber nonlinearity on long-distance transmission," J. Lightwave Technol. **9**, 121–124 (1991).
7. D. Marcuse, "RMS width of pulses in nonlinear dispersive fibers," J. Lightwave Technol. **10**, 17–21 (1992).
8. P. A. Bélanger and N. Bélanger, "Rms characteristics of pulses in nonlinear dispersive lossy fibers," Opt. Commun. **117**, 56–60 (1995).
9. Y. Kodama and S. Wabnitz, "Analytical theory of guiding center NRZ and RZ signal transmission in normally dispersive nonlinear optical fibers," Opt. Lett. **20**, 2291–2293 (1995).
10. Y. Kodama, A. Maruta, and S. Wabnitz, "Minimum channel spacing in wavelength-division-multiplexing nonreturn-to-zero optical fiber transmissions," Opt. Lett. **21**, 1815–1817 (1996).
11. Y. Kodama, S. Wabnitz, and K. Tanaka, "Control of nonreturn-to-zero signal distortion by nonlinear gain," Opt. Lett. **21**, 719–721 (1996).
12. E. Desurvire, *Erbium-Doped Fiber Amplifiers* (Wiley, New York, 1994).
13. A. Hasegawa and Y. Kodama, *Solitons in Optical Communications* (Oxford University, Oxford, UK, 1995).
14. A. Mecozzi, J. D. Moores, H. A. Haus, and Y. Lai, "Soliton transmission control," Opt. Lett. **16**, 1841–1843 (1991).
15. Y. Kodama and A. Hasegawa, "Generation of asymptotically stable optical soliton and suppression of the Gordon–Haus effect," Opt. Lett. **17**, 31–33 (1992).
16. L. M. Hocking and K. Stewartson, "On the nonlinear response of a marginally unstable plane parallel flow to a two dimensional disturbance," Proc. R. Soc. London, Ser. A **326**, 289–313 (1972).
17. N. R. Pereira and L. Stenflo, "Nonlinear Schroedinger equation including growth and damping," Phys. Fluids **20**, 1733–1734 (1977).
18. K. Nozaki and N. Bekki, "Pattern selection and spatiotemporal transition in the Ginzburg–Landau equation," Phys. Rev. Lett. **51**, 2171–2174 (1983).
19. K. Nozaki and N. Bekki, "Exact solutions of the generalized Ginzburg–Landau equation," J. Phys. Soc. Jpn. **53**, 1581–1582 (1984).
20. B. A. Malomed and H. G. Winful, "Stable solitons in two-component active systems," Phys. Rev. E **53**, 5365–5368 (1996).
21. J. Atai and B. A. Malomed, "Stability and interactions of solitons in two-component active systems," Phys. Rev. E **54**, 4371–4374 (1996).
22. N. Efremidis, K. Hizanidis, B. A. Malomed, H. E. Nistazakis, and D. J. Frantzeskakis, "Stabilizing the Pereira–Stenflo solitons in nonlinear optical fibers," Phys. Scr. **T84**, 18–21 (2000).
23. N. Efremidis, K. Hizanidis, B. A. Malomed, H. E. Nistazakis, and D. J. Frantzeskakis, "Stable transmission of solitons in the region of normal dispersion," J. Opt. Soc. Am. B **17**, 952–958 (2000).
24. K. Hizanidis, N. Efremidis, A. Stavdas, D. J. Frantzeskakis, H. E. Nistazakis, and B. A. Malomed, "TDM and WDM with chirped solitons in optical transmission systems with distributed amplification," in *New Trends in Optical Soliton Transmission Systems*, A. Hasegawa, ed. (Kluwer Academic, Dordrecht, the Netherlands, 2000), pp. 139–160.
25. S. P. Craig-Ryan, B. J. Ainslie, and C. A. Millar, "Fabrication of long length of low excess loss erbium-doped optical fibre," Electron. Lett. **26**, 185–186 (1990).
26. J. R. Simpson, L. F. Mollenauer, K. S. Kranz, P. J. Lemaire, N. A. Olsson, H. T. Shang, and P. C. Becker, "A distributed erbium-doped fiber amplifier," in *Optical Fiber Communica-*

tion, Vol. 1 of 1990 Technical Digest Series (Optical Society of America, Washington, D.C., 1990), paper PD19.
27. J. R. Simpson, H. T. Shang, L. F. Mollenauer, N. A. Olsson, P. C. Becker, K. S. Kranz, P. J. Lemaire, and M. J. Neubelt, "Performance of a distributed erbium-doped dispersion-shifted fiber amplifier," J. Lightwave Technol. **9**, 228–233 (1991).
28. J. Atai and B. A. Malomed, "Exact stable pulses in asymmetric linearly coupled Ginzburg–Landau equations," Phys. Lett. A **246**, 412–422 (1998).
29. A. Hasegawa, "Generation of a train of soliton pulses by induced modulational instability in optical fibers," Opt. Lett. **9**, 288–290 (1984).
30. K. Tai, A. Tomita, and A. Hasegawa, "Observation of modulational instability in optical fibers," Phys. Rev. Lett. **56**, 135–138 (1986).